ISPRS Journal of Photogrammetry and Remote Sensing 148 (2019) 197–207

Contents lists available at ScienceDirect

ISPRS Journal of Photogrammetry and Remote Sensing

journal homepage: www.elsevier.com/locate/isprsjprs

Another look on region merging procedure from seed region shift for high-resolution remote sensing image segmentation

Xueliang Zhang[a,b,c], Pengfeng Xiao[a,b,c,*], Xuezhi Feng[a,b,c], Guangjun He[d]

[a] Department of Geographic Information Science, School of Geography and Ocean Science, Nanjing University, Nanjing, Jiangsu 210023, China
[b] Collaborative Innovation Center of South China Sea Studies, Nanjing, Jiangsu 210023, China
[c] Jiangsu Center for Collaborative Innovation in Geographical Information Resource Development and Application, Nanjing, Jiangsu 210023, China
[d] State Key Laboratory of Space-Ground Integrated Information Technology, Beijing 10086, China

ARTICLE INFO

Keywords:
High-resolution remote sensing
Image segmentation
Region merging
Seed region
Geographic object-based image analysis

ABSTRACT

Region merging method is widely used for remote sensing image segmentation in Geographic Object-Based Image Analysis (GEOBIA) because of its simplicity and effectiveness. Instead of improving the merging strategy, similarity measure, and stopping rule for region merging method as usual, we aim at exploring the effectiveness of the seed region shift on region merging-based segmentation. Different region merging procedures with different seed region shift frequencies are compared by fixing other conditions, demonstrating that the shift of seed regions serves as one of the key impacts to segmentation accuracy for region merging method. If the seed regions keep fixed during region merging procedure, it will lead to uneven expansion of regions and consequently low segmentation accuracy. However, if the seed regions can be dynamically shifted during region merging procedure, it will lead to even expansion of regions and achieve similar segmentation performance for different region merging strategies. The findings could be beneficial to selecting or further improving image segmentation method for GEOBIA.

1. Introduction

Geographic Object-Based Image Analysis (GEOBIA) performs remote sensing image analysis on the basic units of image objects, which represent "meaningful" geographic entities or phenomena at multiple scales (Chen et al., 2018). GEOBIA has become the mainstream approach for dealing with high-resolution remote sensing images as image objects can provide abundant geometric features and spectral statistics, as well as spatial context for image analysis (Blaschke 2010; Blaschke et al., 2014). Image segmentation refers to a key step in GEOBIA by producing segments as image objects, on which the GEOBIA performance is highly depended (Ma et al., 2017).

Image segmentation aims at partitioning an image into perceptually homogeneous and spatially contiguous regions, where each region consists of a set of adjacent pixels (Dey et al., 2010). In the remote sensing community, the region-based segmentation method is widely used as it can inherently provide complete region segments for successive object-based analysis, while the edge-based segmentation method is usually preferred to improve the boundary accuracy for region-based segmentation (Chen et al., 2012; Li et al., 2010). To perform region-based segmentation, we can either gradually partition the image into smaller regions until the stopping rule is met by, e.g. graph cut (Shi and Malik, 2000) and splitting (Wuest and Zhang, 2009), or gradually expand regions from the initial state of pixels by, e.g. clustering (Comaniciu and Meer, 2002; Huang and Zhang, 2008; Wang et al., 2018) and merging (Baatz and Schäpe, 2000; Castilla et al., 2008; Tilton et al., 2012).

Because of the improvement of spatial resolution, the heterogeneity among geographic objects is seriously increased in high-resolution remote sensing images, resulting in that a single segmentation is difficult to accurately separate various objects (Benz et al., 2004). Hence, a basic requirement for remote sensing image segmentation is being able to provide multiscale segmentations for describing various objects or even for delineating objects at different semantic levels. Among the region-based segmentation methods, the region merging method is convenient to provide multiscale segmentations by simply setting different stopping rules, where more merging iterations could lead to coarser segments, and vice versa. Another benefit provided by region merging method is to produce nested multiscale segments (Zhang et al., 2013), which can avoid boundary conflicts across segmentation scales for successive multiscale analysis. A key problem coming with multiscale segmentation is to automatically optimize the segmentation scale

* Corresponding author at: Department of Geographic Information Science, School of Geography and Ocean Science, Nanjing University, China.
E-mail address: xiaopf@nju.edu.cn (P. Xiao).

https://doi.org/10.1016/j.isprsjprs.2019.01.007
Received 4 September 2018; Received in revised form 7 December 2018; Accepted 8 January 2019

parameter for specific applications (Hay et al., 2005). A lot of efforts have been paid into this topic to select meaningful/optimal segmentation scale(s) (Drăguţ et al., 2014; Ming et al., 2015) or to fuse multiscale segments (Bruzzone and Carlin, 2006; Johnson and Xie, 2011). However, the segmentation algorithm itself is still far from ideal and improvement of segmentation performance remains a challenging problem.

Specifically considering the widely-used region merging method for remote sensing image segmentation, the performance improvement mainly comes from three aspects: merging cost, merging strategy, and stopping rule. The merging cost, also referring to the similarity measure, quantifies the similarity between adjacent regions and achieves segmentation performance improvement by utilizing abundant region features, e.g. spectral (Yang et al., 2017), textural (Trias-Sanz et al., 2008), structural (Akçay and Aksoy, 2008, Liu et al., 2015), shape (Baatz and Schäpe, 2000; Shackelford and Davis, 2003), and edge (Wang et al., 2017; Yu and Clausi, 2008) features. The merging strategy determines how to search the region pairs to be merged, which is directly related to the optimization strength. The local best merging (LBM) (Castilla et al., 2008), local mutual-best merging (LMM) (Baatz and Schäpe, 2000), and global best merging (GBM) (Beaulieu and Goldberg, 1989) strategies are widely used. The searching space and thus the theoretical optimization strength increases from LBM to GBM. Examples of improving merging strategies include combining region merging with spectral clustering (Tilton et al., 2012) and combining both global- and local-oriented region merging strategies (Zhang et al., 2014). In terms of stopping rule, usually a global threshold is set for the whole image, while recent studies try to set locally adaptive thresholds to deal with the great heterogeneity in images (Yang et al., 2017; Hu et al., 2017).

Even though plenty of efforts have been paid to improving region merging method for remote sensing image segmentation, the effectiveness of the status of the seed regions on region merging is almost neglected. A seed region is described as the region getting expanded during region merging procedure, which is similar as a seed in region growing procedure. In seeded region growing procedure, the seeds are firstly assigned and then gradually growing by merging neighboring pixels (Adams and Bischof, 1994). A proper assignment of seeds is crucial for the success of region growing (Shih and Cheng, 2005). For example, the watershed transform method could be viewed as a special region growing method, in which too many seeds could result in seriously over-segmentation and the markers are usually needed to extract meaningful seeds (Xiao et al., 2010).

Unlike rigid seeds in seeded region growing, the seed regions could be dynamically shifted during region merging procedure. A previous study proposed to determine the order of picking seed regions for merging was according to the rule of making successive seed regions as far as possible (Baatz and Schäpe, 2000). In this study, instead of focusing on the picking order of seed regions, we will evaluate the effectiveness of seed region shift on region merging-based segmentation and further quantifies the effectiveness. Specifically, we will first give an insight on how seed regions are shifted during segmentation procedure for different merging strategies, including LBM, LMM, and GBM, as well as their variants with the constraint of shifting seed regions. Then we will evaluate how the shift of seed regions could influence the segmentation performance by fixing other conditions. Finally, the effectiveness of shift frequency on segmentation accuracy will be further quantified. To our knowledge, it is the first time to understand region merging-based segmentation method from the shift of seed regions. We will demonstrate that it serves as a key factor to the success of region merging-based segmentation to make the seed regions shift dynamically, which can help us better understanding the region merging procedure and could be beneficial for further improvement.

The rest of this paper is organized as follows. The shift of seed regions in different merging procedures are detailedly analysed and compared in Section 2. The influence of the seed region shift on segmentation results is experimentally evaluated and discussed in Section 3. Finally, conclusions are drawn in Section 4.

2. Methodology

2.1. Region merging procedure

The region merging-based segmentation is performed on a graph model built on initial over-segmentation. Initial segmentation is optional because the graph model can be built on either initial segments or original pixels. We prefer to perform initial segmentation at first, which should be apparently over-segmented and can thus preserve real boundaries very well. The number of initial segments is apparently smaller than that of original pixels, which can help to reduce the number of nodes in graph model and consequently relieve both the computing and memory burdens. The real boundaries are well preserved so that the initial segmentation will not do harm to the successive region merging procedure by introducing under-segmentation errors. A region growing method is used for producing initial segmentation in this study (Zhang et al., 2013), and other methods could also be used, e.g. watershed transform (Vincent and Soille, 1991) and superpixel clustering (Liu et al., 2018).

The graph model, including both region adjacency graph (RAG) (Felzenszwalb and Huttenlocher, 2004) and nearest neighbor graph (NNG) (Haris et al., 1998) is then constructed on initial segmentation. The nodes in RAG represent each initial segment and the arcs record the adjacency relationship between nodes. The arc weight is calculated according to the similarity measure between two adjacent nodes. The similarity measure integrates region features of size (a), spectral standard deviation change ($CStd$), shape change ($CCmp$), and edge penalty ($g(ES)$) (Zhang et al., 2014), as shown in Eq. (1), where ω is a weight parameter and set as 0.5 by default. The lower arc weight indicates the higher similarity between two regions. The benefit of NNG is to accelerate searching the best neighbor during region merging procedure by recording the nearest neighboring node of each node in the graph.

$$M = (a_1 + a_2)(\omega \cdot CStd + (1 - \omega)CCmp)g(ES). \tag{1}$$

Three different region merging strategies, including LBM, LMM, and GBM, are applied on the same graph model for comparison, and the specific region merging workflow for each strategy are shown in Fig. 1. The stopping rule is set as the threshold of region similarity for different merging strategies. When all the arc weights are higher than the threshold, the region merging procedure stops. In the global-oriented region merging procedure GBM, the most similar pair of adjacent regions in the whole image is searched for merging at each iteration. While in local-oriented region merging procedure of LBM and LMM, only the best neighbor and mutual best neighbor is respectively searched for merging, which results in apparently lower searching burden than GBM. Comparing LBM with LMM, LBM only needs to search the best neighbor from all its neighbors, while in addition to this, LMM has to search all the neighbors of its best neighbor to determine whether they are mutual best. Even though the searching space of LMM is larger than that of LBM, the computation complexity for searching is similar with the benefit of NNG. As a whole, the optimization strength is successively decreasing from GBM, LMM, to LBM as the searching space is compressed accordingly.

2.2. Seed region shift for different merging strategies

During region merging procedure, a seed region is gradually expanded by merging its neighboring regions from the initial state to the final state that is defined by the stopping rule. If the seed region keeps merging its neighbors until reaching the final state, it is viewed as fixed or not shifted. However, if a seed region is refused to merge its neighbors when it does not reach the final state and transfers to another seed region, it is defined as shifted.

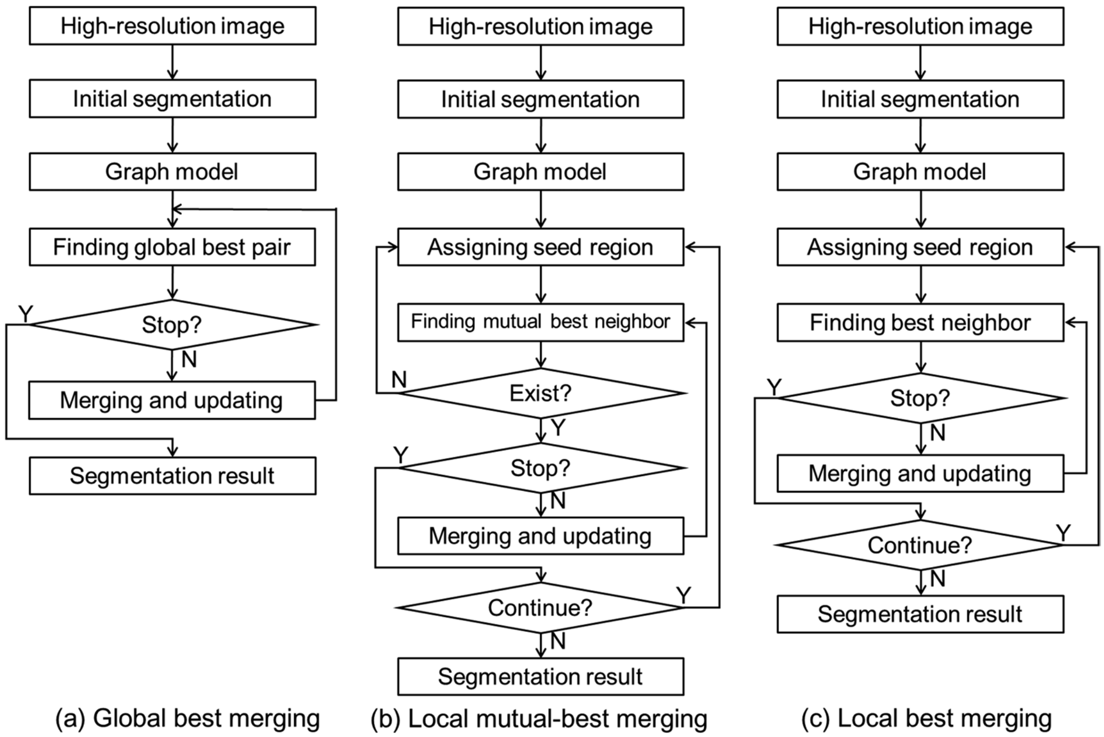

Fig. 1. Flow diagram of region merging-based remote sensing image segmentation based on different merging strategies.

The shift of seed regions is different for different region merging strategies. In terms of the GBM strategy, since the globally most similar pair is selected for merging at each iteration, the seed region is inherently determined by the merging order and thus could be theoretically shifted after each iteration. Accordingly, we do not need to explicitly assign seed region for GBM because seed region is actually assigned implicitly by GBM.

The shifts of seed regions for local-oriented region merging methods LBM and LMM are not as frequent as those for GBM. We need to explicitly assign seed region for LBM and LMM as shown in Fig. 1(b) and (c), which is randomly assigned in this study. The seed region shifts between LBM and LMM are also different, as shown in Fig. 2. During the merging procedure of LBM, the seed region will not shift because it keeps merging best neighbors until meeting the stopping rule. However, only mutual best neighbors are allowed to be merged during LMM procedure, which could lead to the shift of seed regions before reaching the final state. For a seed region, even though the similarity with its best neighbor is greater than the threshold, the merging could still be refused by LMM if the mutual best requirement is not satisfied and thus transfers to another seed region. Hence, we can know that the shift frequency of seed regions is decreased from GBM, LMM, to LBM, specifically from per iteration, per several iterations, to no-shift, which should be related to the gradually compressed searching space among the different merging strategies.

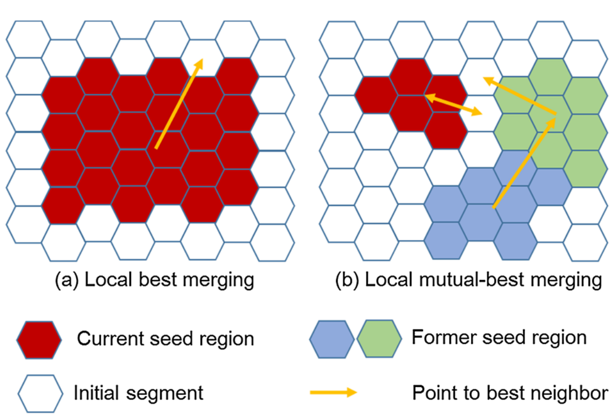

Fig. 2. A comparison of region merging procedures in terms of the shift of seed regions between LBM (no-shift) and LMM (per several iterations), where the seed region keeps merging its best neighbors in LBM, while the seed region would shift if the mutual best constraint is not satisfied in LMM.

To further illustrate the influence caused by the shift of seed region, the step-wise scale parameter (SWSP) strategy is introduced to create more situations in terms of the shift frequency. SWSP is originally designed for constraining local-oriented region merging to produce nested multiscale segmentations (Zhang et al., 2013). The basic idea of SWSP is to use a set of gradually increased scale parameters $\{S \mid S_1, S_2, \ldots, S_k$, where $S_1 < S_2 < \ldots < S_k\}$ to control region merging. Controlled by SWSP, the merging iterations at S_i are performed on the output at the finer segmentation scale $S_{i\text{-}1}$, resulting in nested multiscale segmentations. Instead of producing k nested segmentation scales as described by (Zhang et al., 2013), we make use of SWSP to produce the target segmentation with scale parameter S_k, which helps to create more situations for seed region shift.

The region merging procedure constrained by SWSP to produce the target segmentation S_k is shown in Fig. 3. The scale parameter S_i is set with the same increasing step and equals to *step* × *i*, where *step* is set as 5 by default. It is directly related to the threshold of region similarity. Specifically, the threshold at scale i is equal to $(S_i)^2$. Hence, the set of scale parameters serves as a set of gradually increased threshold values. During the region merging procedure, the graph model is timely updated after each merging iteration as shown in Fig. 1. In terms of the region merging procedure constrained by SWSP, the region merging at scale S_i is successively performed on the timely updated graph model corresponding to segmentation scale $S_{i\text{-}1}$, until reaching the target segmentation scale S_k.

SWSP forces the seed region to shift at each segmentation scale with the benefit of region merging scale by scale. Specifically at scale i, the region merging for a seed region will be refused if the similarity measure is higher than $(S_i)^2$ and then return to merging at coarser segmentation scales. In this case, the seed region is thus forced to shift. The

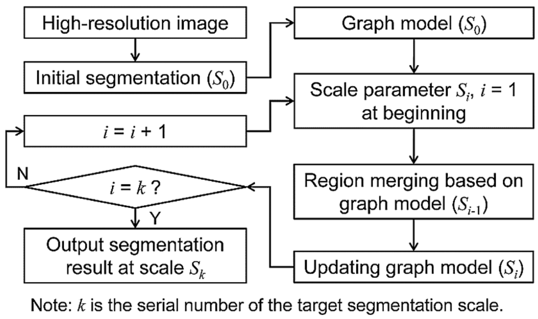

Fig. 3. Flow diagram of region merging-based segmentation procedure constrained by step-wise scale parameter (SWSP).

shift frequency of GBM is both per iteration with or without SWSP constraint because the seed region is implicitly assigned by GBM itself at each merging iteration. However, the shift frequency of LMM would be increased with SWSP constraint because the seed regions are forced to shift at each scale in addition to the shift constrained by mutual best requirement, but it is still per several iterations. The frequency of LBM is not no-shift any more, but to shift k-1 times because the seed regions are forced to shift at each scale in SWSP.

The seed region shift frequencies for the different region merging procedures and the corresponding constraints for shifting are presented in Table 1. To demonstrate the effectiveness of seed region shift on region merging-based segmentation, four sets of comparisons are designed based on the three merging strategies GBM, LMM, and LBM with or without SWSP. The comparisons include: (1) comparing the three strategies without SWSP to reveal the effectiveness caused by seed regions with no-shift, shift per several iterations and shift per iteration; (2) comparing the three strategies with SWSP to reveal the effectiveness caused by different seed region shift frequencies; (3) comparing the two cases of with and without SWSP for each merging strategy to reveal the effectiveness of increasing seed region shift frequency; (4) comparing different situations of LBM + SWSP by setting different *step* values in SWSP to quantify the effectiveness of seed region shift frequency. The comparisons of (1) and (2) may reveal the effectiveness of different optimization strengths in addition to the different seed region shifts by comparing different merging strategies. However, the comparison (3) would purely reveal the effectiveness of seed region shifting frequencies because the same merging strategy is for comparison. Hence, by combining the comparisons (1) and (2) with the comparison (3), we can get an insight to the relative importance of seed region shift in comparison to optimization strength. The comparison results will be presented in the following section.

2.3. Segmentation evaluation

The supervised evaluation strategy is adopted to quantitatively evaluate the segmentation differences caused by seed region shift. The evaluation measures that could reveal the overall segmentation accuracy are adopted (Costa et al., 2018), specifically including the *F*-measure (Zhang et al., 2015), bidirectional consistency error (Martin, 2003), and symmetric partition distance (Cardoso and Corte-Real, 2005). Through experimental tests, the three measures show a similar trend to reveal the segmentation differences caused by seed region shift. Hence, we would present the evaluation results by *F*-measure. At first, the *precision* measure and the *recall* measure are separately calculated as Eqs. (2) and (3) by overlaying the segmentation result with the reference. Seg_i and Ref_i represent a segment and a reference object in the segmentation result and the reference, respectively. Ref_{imax} and Seg_{imax} represent the reference object and the segment that has the largest overlapping area with Seg_i and Ref_i, respectively. The *precision* and *recall* measures can reflect the over- and under-segmentation errors, where a high *precision* value combining with a low *recall* value indicate over-segmentation while a high *recall* value combining with a low *precision* value indicate under-segmentation. The *F*-measure is calculated by combining *precision* and *recall* measures to reveal the overall segmentation accuracy. A higher *F*-measure value indicates a better segmentation quality.

$$precision = \frac{\sum_{i=1}^{n} |Seg_i \cap Ref_{imax}|}{\sum_{i=1}^{n} |Seg_i|}, \tag{2}$$

$$recall = \frac{\sum_{i=1}^{m} |Ref_i \cap Seg_{imax}|}{\sum_{i=1}^{m} |Ref_i|}, \tag{3}$$

$$F\text{-measure} = \frac{2 \times precision \times recall}{precision + recall}. \tag{4}$$

3. Experiments and discussions

Different merging strategies are performed and compared to reveal the segmentation differences caused by seed region shift, where the initial segmentation, graph model, similarity measure, and stopping rule are set the same for different merging procedures. The segmentation differences are quantitatively evaluated to demonstrate the influence of the shift of seed regions in terms of the number of segments in the result, segmentation accuracy, and segmentation time. How the region merging procedure, e.g. the even/uneven expansion of regions, is influenced by seed region shift is also reflected from the differences. Furthermore, how frequent the seed region shift should be to ensure segmentation success is quantitatively assessed.

3.1. Datasets

A QuickBird image in Hangzhou City, China is used for experiment to demonstrate the influence of seed region shift on region merging-based segmentation. The image consists of four spectral bands: blue, green, red, and near infrared. The spatial resolution is improved to 0.6 m after pansharpening (Zhang, 2002). Four subsets in this image are used to present the segmentation results and named as T1–T4, as shown in Fig. 4. The four test images show the landscapes of industrial area, farmland area, residential area, and watery area, respectively. The segmentation references for the test images are manually delineated by specialists in remote sensing and reviewed by others to catch any obvious errors. Finally, there are 292, 156, 554, and 107 reference segments for T1–T4, respectively.

Table 1
Shift frequencies of seed regions for presented different region merging procedures and the corresponding constraints leading to shift.

Region merging procedure	Seed region shift frequency	Constraints for shift
LBM	No shift	No constraint
LMM	Shift per several iterations	Local mutual-best constraint
GBM	Shift per iteration	Global-best constraint
LBM + SWSP	Shift k-1 times	SWSP
LMM + SWSP	Shift per several iterations but higher than that of LMM	Local mutual-best constraint + SWSP
GBM + SWSP	Shift per iteration	Global-best constraint + SWSP

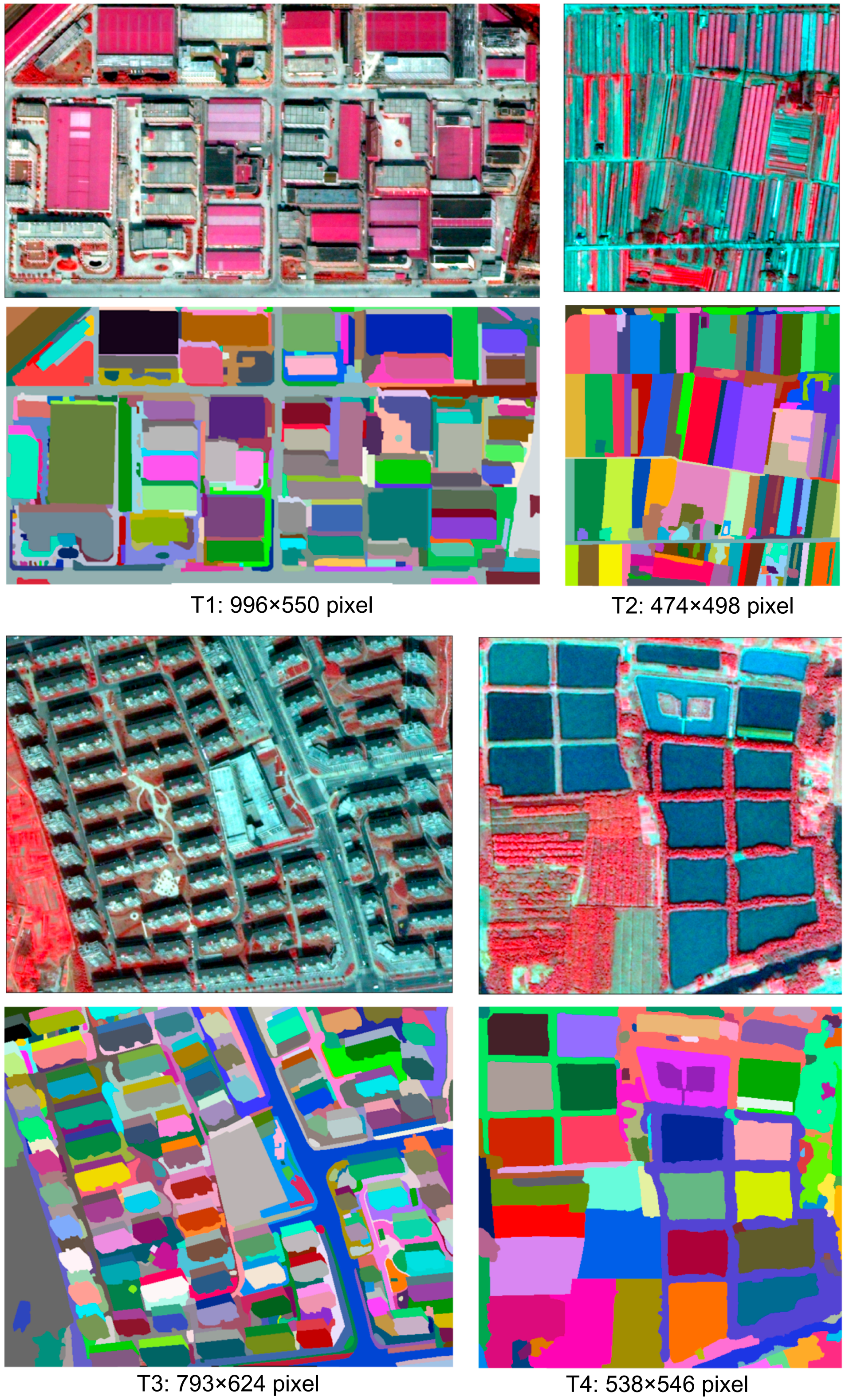

Fig. 4. Test images and references for experiments. Original images are shown with band combination of near infrared, red, and green bands. The different colors in references represent distinct segments without semantic meanings. (For interpretation of the references to color in this figure legend, the reader is referred to the web version of this article.)

3.2. Segment number impacted by seed regions

Before evaluating segmentation accuracy, the difference of segment number caused by seed region shift is first evaluated, which could help to reveal the different region merging procedures caused by seed region shift.

At first, the same similarity threshold is set for region merging methods GBM, LMM, and LBM. The number of segments produced by each method is shown in Table 2. Generally, given the same similarity threshold, the number of segments is decreased from GBM, LMM, to

Table 2
Number of segments produced by different region merging strategies.

Threshold	Number of segments											
	T1			T2			T3			T4		
	GBM	LMM	LBM	GBM	LMM	LBM	GBM	LMM	LBM	GBM	LMM	LBM
1000	1106	1064	431	491	494	182	1079	1048	437	372	386	150
2000	677	647	179	292	290	50	645	624	143	228	226	67
3000	503	482	78	210	201	15	495	479	66	177	181	41

LBM with the decrease of shift frequency of seed region. The segment number between GBM and LMM is similar with each other, which shows that there is not much difference caused by shift frequency of seed region between per iteration and per several iterations. However, the segment number for LBM is apparently smaller than that for GBM and LMM, which reflects a huge difference between shifted and non-shifted seed regions.

It may be doubted that the segment number difference among different region merging strategies is caused by the optimization searching space in addition to the seed region shift. To illustrate this, the segment number for each merging strategy with SWSP constraint are presented in Table 3. It is noted that the scale parameter in SWSP actually serves as the similarity threshold to control the stop of region merging, where the threshold is equal to the square of the scale parameter. With the SWSP constraint, the seed region of LBM is forced to shift, while the optimization searching space is still same as that without SWSP. From Table 3, it can be seen that the segment number still keeps decreasing from GBM, LMM, to LBM with the decrease of shift frequency of seed region. However, the difference between LBM and LMM, GBM is slight. Comparing the differences in Tables 2 and 3, it demonstrates that the segment number difference should be related to seed region shift. Specifically, different optimization strengths among different merging strategies would not cause much difference in segment number as long as the seed region is shifted, while it would lead to great difference between shifted and non-shifted seed region.

Why the segment number is influenced by the seed region shift and what is the corresponding effect on segmentation result? If the seed region is not shifted, it keeps expanding by merging neighbors while its neighbors remain unchanged as the initial segments during the merging procedure. We call this as uneven expansion. However, if the seed region is shifted, its expansion tends to terminate after several merging iterations constrained either by a strong optimization strategy or by SWSP. Then its neighbors could get the chance to expand before reaching its final state. Accordingly, when it comes back to the seed region to continue expansion, its neighbors have been expanded rather than remain non-changed. We call this as even expansion. According to Tables 2 and 3, when setting the same similarity threshold, the uneven expansion of LBM results in much smaller segment number than that for even expansion. In other words, when the segment number is the same in segmentation results, the similarity threshold for uneven expansion should be smaller than that for even expansion, which means that the similarity between adjacent segments produced by uneven expansion is higher than that by even expansion according to the definition of the similarity measure in Eq. (1). Hence, when setting the same similarity threshold, the uneven expansion results in fewer segments because the similarity between adjacent segments is higher than that for even expansion. The higher similarity between adjacent segments should be related to the lower heterogeneity among regions. According to the criterion of good segmentation quality for unsupervised segmentation evaluation, which requires segments having both high inner homogeneity and inter heterogeneity (Zhang et al., 2008), the uneven expansion may lead to poorer segmentation quality than even expansion because of the lower heterogeneity among regions. The following supervised evaluation results would demonstrate this.

3.3. Segmentation accuracy impacted by seed regions

As discussed above, the uneven expansion caused by non-shifted seed regions would result in poorer segmentation performance than the even expansion by shifted seed regions. The supervised evaluation results are presented to demonstrate this.

The segmentation results from different region merging strategies without SWSP are first evaluated using *F*-measure and presented in Fig. 5. In order to avoid the uncertainty of over- or under-segmentation errors caused by different number of segments, the segmentation results from different merging strategies are with similar segment number for comparison. In this case, the similarity threshold values are set different for different merging strategies. Three segmentation scales are presented for comparison, ranging from over-, medium-, to under-segmentation according to visual inspection. Generally, the segmentation accuracies between GBM and LMM are similar, showing that the shift frequency of seed regions between per iteration and per several iterations does not result in apparent difference on segmentation accuracy.

Comparing the accuracies of LBM with those of GBM and LMM, they are similar or even LBM achieves a bit higher *F*-measure value at the fine segmentation scale, e.g., for image T1 and T2. But the LBM accuracy tends to get lower as the segmentation becomes coarser. This could be owing to the error accumulation caused by the uneven expansion of non-shifted seed region in LBM. At the fine segmentation scale, the similarity threshold is relatively small and the number of the merging iterations is not large. The uneven expansion in LBM could produce several relatively larger segments and thus achieve higher *recall* value

Table 3
Number of segments produced by different region merging strategies with SWSP constraint. The stopping threshold of region merging is equal to the square of the scale parameter.

Scale parameter	Number of segments											
	T1			T2			T3			T4		
	GBM	LMM	LBM	GBM	LMM	LBM	GBM	LMM	LBM	GBM	LMM	LBM
40	776	763	732	340	328	317	762	733	688	271	262	261
80	287	275	269	188	171	159	299	286	282	103	99	99
120	167	166	159	108	99	97	185	173	170	68	65	54
160	106	103	101	51	50	43	113	116	112	41	42	40

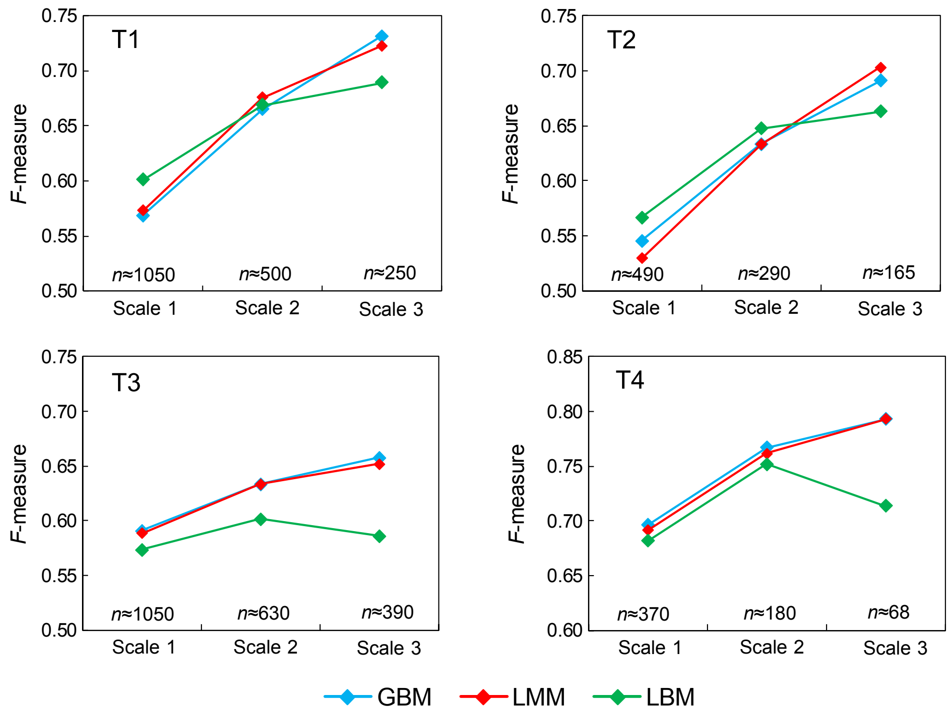

Fig. 5. Segmentation accuracies for different region merging strategies, where *n* represents the number of segments in the segmentation results, the segmentation results from Scale 1 to Scale 3 range from over-, medium-, to under-segmentation according to visual inspection.

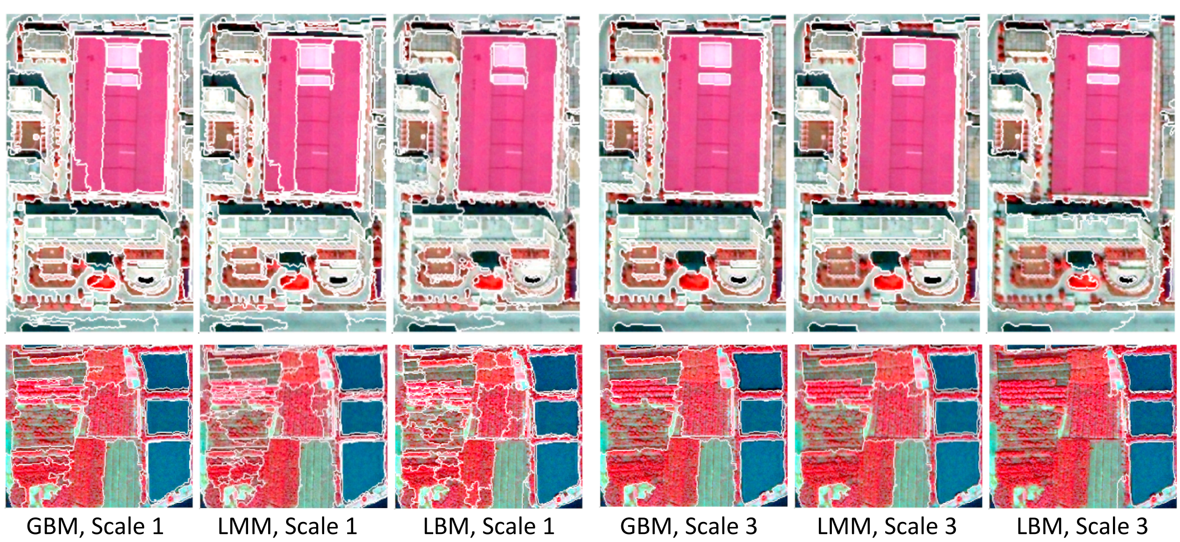

Fig. 6. Visual comparison of segmentation results at relatively fine (Scale 1) and coarse (Scale 3) segmentation scales produced by different region merging strategies. The results in the first and second rows are subsets from image T1 and T4, respectively.

than the even expansion in LMM and GBM, as shown in the T1 fine-scale segmentation results in Fig. 6. This results in the similar or even higher *F*-measure value for LBM when comparing with LMM and GBM. However, when the segmentation scale is coarse, the similarity threshold is accordingly set large. In this case, the uneven expansion in LBM becomes serious because more merging iterations are allowed. This could produce several too large segments while the even expansion in LMM and GBM can correctly segment objects, which results in higher *F*-measure value of LMM and GBM compared with LBM, as shown in the coarse segmentation results of T1 and T4 in Fig. 6.

To further demonstrate the influence of the uneven/even expansion caused by shifted/non-shifted seed region on segmentation accuracy, the segmentation results from different region merging strategies with SWSP constraint are evaluated and presented in Fig. 7. In this case, the seed regions are shifted and thus evenly expanded for all the three region merging strategies, except that the shift frequency is different. The segmentation results from different merging strategies are produced by setting the same segmentation scale parameters because the segment number tends to be similar for different merging strategies with SWSP as analysed in Section 3.2. It can be seen in Fig. 7 that the segmentation accuracies are similar at multiple scales for the three region merging strategies with SWSP. The segmentation results in Fig. 8 further illustrate the similarity. This indicates that the shifted seed region could help to achieve similar segmentation accuracy for different region merging strategies even the optimization ability is different.

According to the above analysis, we can know that once the seed regions are shifted, the segmentation performance could be similar for different merging strategies. A remaining question is that how frequent

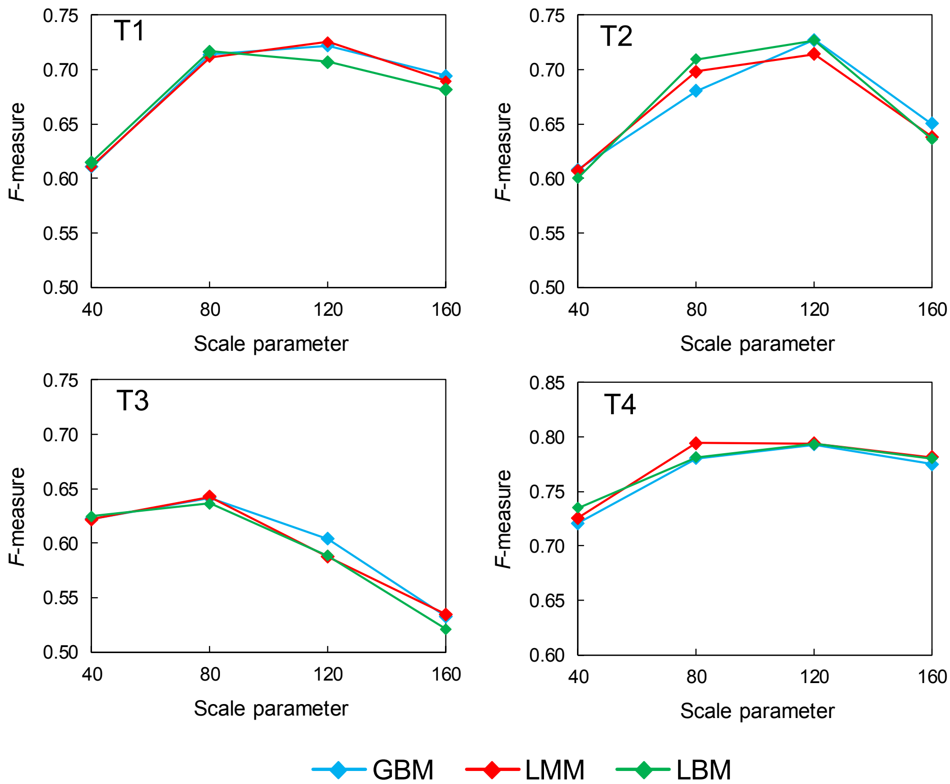

Fig. 7. Segmentation accuracies for different region merging strategies with SWSP constraint.

the seed region should be shifted to ensure similar segmentation performance for different region merging strategies. The performance between GBM and LMM is similar, showing that there is not much difference between per iteration and per several iterations for the shift frequency of seed region. But it is difficult to quantify the "several" for LMM. Hence, to answer this question, the LBM + SWSP strategy is adopted for quantification. Assuming that there are k scale parameters in SWSP, the seed regions would shift $k - 1$ times. Then given a target segmentation scale parameter, we can adjust the increasing step in SWSP and thus to adjust the number of scale parameters, consequently leading to the change of the shift frequency of seed regions.

Specifically, given the target segmentation scale parameter as 80, the increasing step is set from 1 to 40 and the segmentation accuracies by LBM with SWSP constraint are presented in Fig. 8. Accordingly, the number of segmentation scale parameters ranges from 80 to 2, and consequently the frequency of seed region shifts ranges from 79 to 1. It is seen from Fig. 9 that the step values from 1 to 20 could result in similar segmentation accuracies for the test images, where the seed regions shift at least 3 times. However, when the step is set as 40 and the seed regions only shift 1 time, the segmentation accuracies

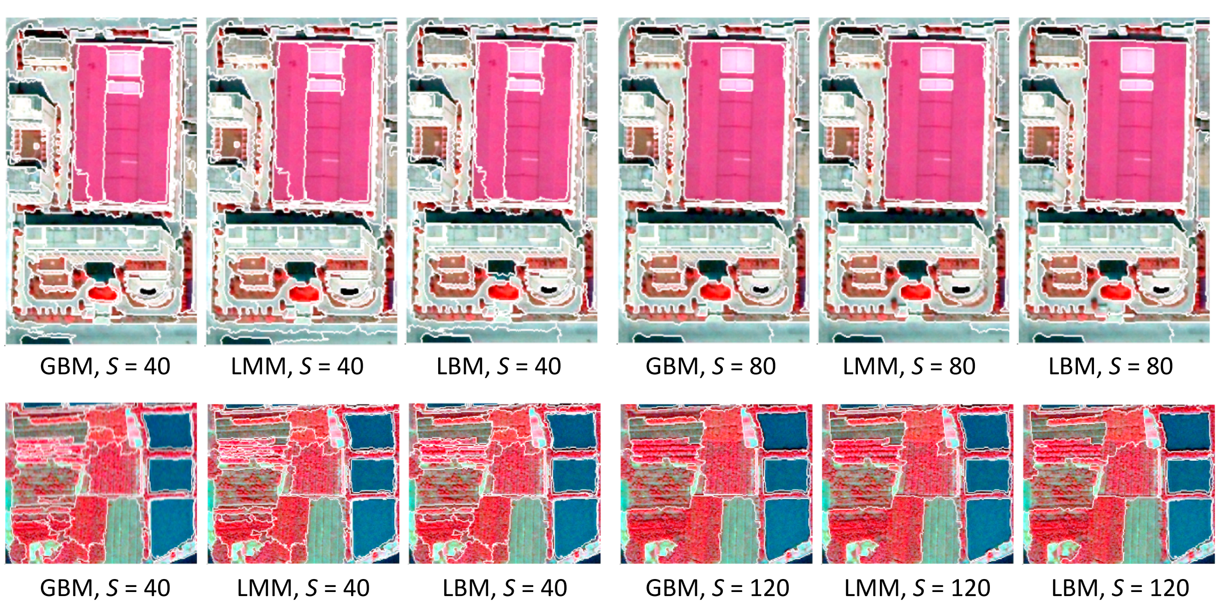

Fig. 8. Visual comparison of segmentation results produced by different region merging strategies with SWSP constraint. The results in the first and second rows are subsets from image T1 and T4, respectively.

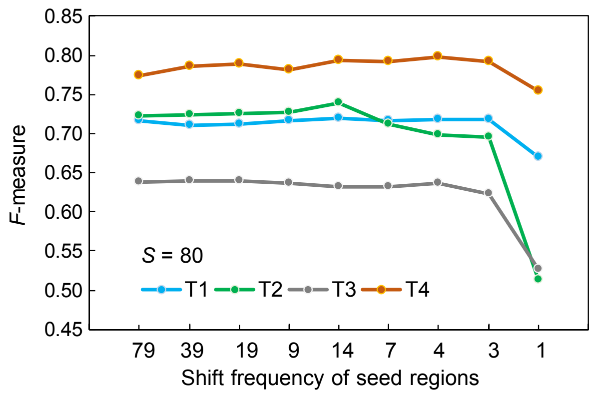

Fig. 9. Segmentation accuracies for region merging strategy LBM + SWSP with different shift frequency of seed regions.

apparently getting lower. The segmentation results in Fig. 10 further illustrate this tendency. As a whole, it indicates that the high shift frequency of seed regions would not do harm to segmentation accuracy for region merging strategy, but it also would not apparently improve segmentation accuracy. However, the too low shift frequency of seed regions could result in lower segmentation accuracy. For safety, it is suggested to shift the seed regions at least 3 times to ensure high segmentation accuracy.

3.4. Segmentation time impacted by seed regions

The segmentation time is determined by the computation complexity of searching the best region that is allowed to be merged into the seed region. Actually, the seed region shift could also influence the segmentation time. Taking the test image T1 as an example, the segmentation time for different region merging strategies without/with SWSP are calculated and presented in Fig. 11.

It can be seen from Fig. 11(a) that the segmentation time of GBM is constantly higher than that of LMM, which is caused by searching the global best pair for merging in GBM. The segmentation time increment of GBM will be further enlarged if the image size is getting larger because more nodes are involved to increase the searching time. As the threshold is setting larger, the segmentation time of GBM and LMM is not apparently increased even though more merging iterations are performed, which is because the number of remaining nodes to be merged is gradually decreased. However, the segmentation time of LBM keeps increasing as the stopping threshold is setting larger. At first, it is same as that of LMM, this shows that the uneven expansion of the seed regions in LBM is still not serious at such a small threshold. As the threshold is getting larger, the uneven expansion becomes more serious. This means that the number of adjacent regions of the seed region is getting larger, which is because the seed regions is very large while its adjacent regions remains small as the initial segments. Hence, it would take more and more time to search the best neighbor to be merged for LBM as more uneven expansion iterations are allowed.

In Fig. 11(b), it can be seen that the segmentation time between LBM and LMM becomes almost same with SWSP constraint, which means that the segmentation time of LBM with SWSP does not keep increasing as that without SWSP. This further shows that the shift of seed regions helps to avoid the uneven expansion of seed region and thus reduce segmentation time. The almost same segmentation time between LBM and LMM with SWSP is owing to the NNG model, which makes the searching complexity of LMM same as that of LBM by recording the best neighbor for each node. Since the shift of seed regions for SWSP is not different with or without SWSP, the segmentation time for GBM in Fig. 11(a) and (b) is not different. However, we can see that the segmentation time of LMM with SWSP in Fig. 11(b) is a bit less than that in Fig. 11(a) without SWSP. This could be owing to the higher shift frequency of seed region for LMM with SWSP than that without SWSP. Once the shift frequency is higher, the expansion of seed region would terminate earlier and thus the number of its neighbors is smaller, which results in less time for searching.

4. Conclusions

In this study, we take another look on region merging strategies for high-resolution remote sensing image segmentation from the shift of seed regions. The three widely-used region merging strategies GBM, LMM, and LBM, as well as the SWSP constraint are adopted to create different seed region shift frequencies for comparison. The segmentation differences caused by seed region shift are quantified in terms of both segmentation accuracy and time to demonstrate the impact.

The results demonstrate that the shift of seed regions serves as one of the key factors to ensure segmentation accuracy for region merging method. Without seed region shift, the seed region would be unevenly

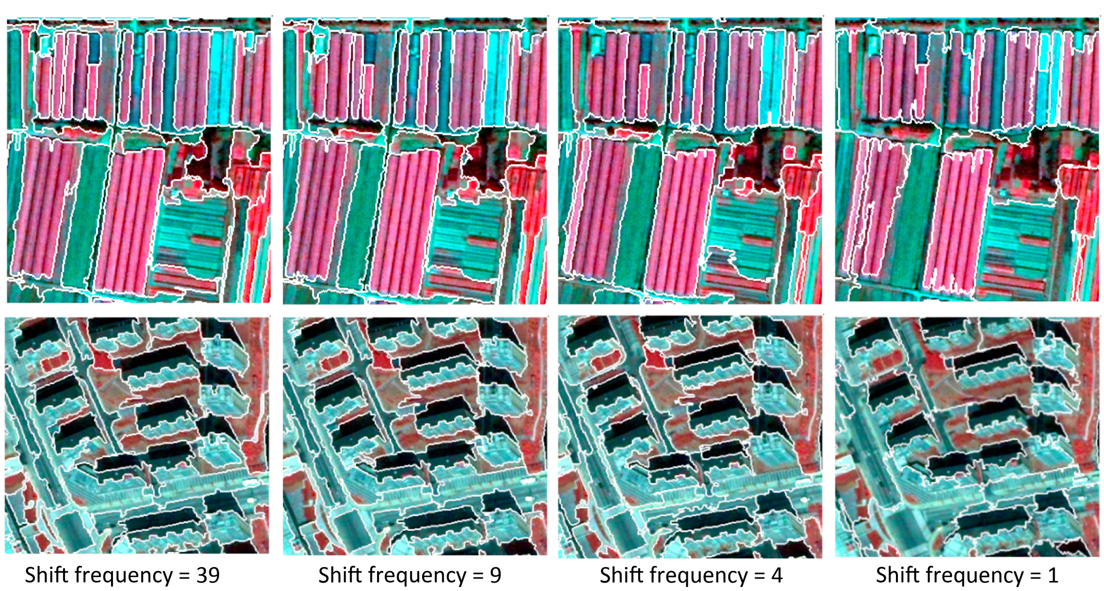

Fig. 10. Segmentation results from region merging strategy LBM with SWSP constraint at *scale* 80 by setting different shift frequency of seed regions. The results in the first and second rows are subsets from image T2 and T3, respectively.

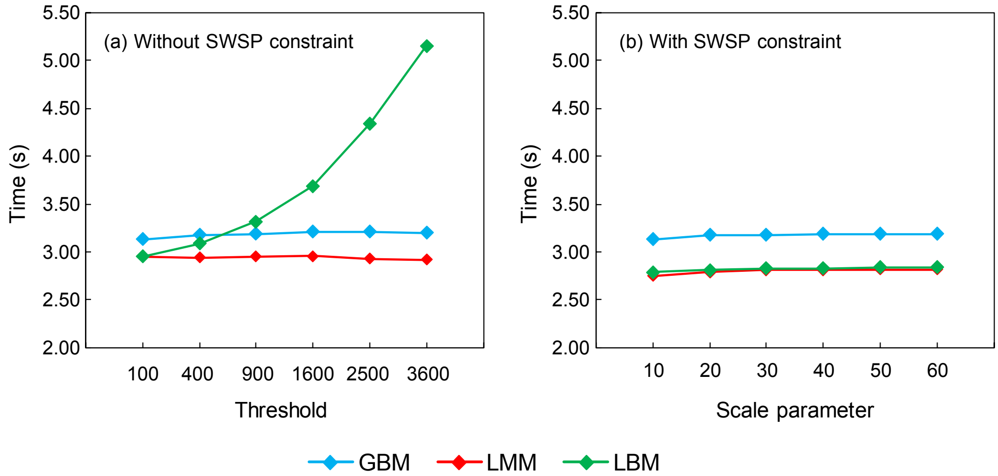

Fig. 11. Segmentation time for different region merging strategies considering seed region shift by taking test image T1 as an example.

expanded, which could result in lower segmentation accuracy and more segmentation time, especially when the segmentation scale is getting coarse and more merging iterations are allowed. It is demonstrated that once the seed regions are shifted several times, safely more than 3 times, the segmentation accuracy tends to be similar even using different merging strategies with different optimization strengths. It is also demonstrated that once the shift frequency of seed regions is large enough, higher shift frequency would not do harm to the segmentation accuracy, and it also could not improve the segmentation accuracy.

Even though this study does not directly improve region merging-based segmentation for remote sensing images, it provides a deep understanding to the region merging procedure and makes us aware of the key factor of seed region shift that influences segmentation performance for the widely used region merging method. This could be beneficial to segmentation method selection and further improvement of segmentation performance by region merging in the future.

Acknowledgement

This work was supported by the National Natural Science Foundation of China (Grant Nos. 41601366, 41871235), the National Science and Technology Major Project of China (Grant No. 21-Y20A06-9001-17/18), the Natural Science Foundation of Jiangsu Province (Grant No. BK20160623), the Open Research Fund of State Key Laboratory of Space-Ground Integrated Information Technology (Grant No. 2016_SGIIT_KFJJ_YG_01), and the Fundamental Research Funds for the Central Universities (Grant No. 020914380040). The authors would like to thank the anonymous reviewers and editors for their comments to improve the paper.

References

Adams, R., Bischof, L., 1994. Seeded region growing. IEEE Trans. Patt. Anal. Mach. Intell. 16 (6), 641–647.
Akçay, H.G., Aksoy, S., 2008. Automatic detection of geospatial objects using multiple hierarchical segmentations. IEEE Trans. Geosci. Rem. Sens. 46 (7), 2097–2111.
Baatz, M., Schäpe, A., 2000. Multiresolution segmentation-an optimization approach for high quality multi-scale image segmentation. In: Strobl, J., Blaschke, T., Griesebner, G. (Eds.), Angewandte Geographische Informations-Verarbeitung XII. Wichmann Verlag, Karlsruhe, pp. 12–23.
Beaulieu, J.M., Goldberg, M., 1989. Hierarchy in picture segmentation: a stepwise optimization approach. IEEE Trans. Patt. Anal. Mach. Intell. 11 (2), 150–163.
Benz, U.C., Hofmann, P., Willhauck, G., Lingenfelder, I., Heynen, M., 2004. Multi-resolution, object-oriented fuzzy analysis of remote sensing data for GIS-ready information. ISPRS J. Photogramm. Rem. Sens. 58 (3–4), 239–258.
Blaschke, T., 2010. Object based image analysis for remote sensing. ISPRS J. Photogramm. Rem. Sens. 65 (1), 2–16.
Blaschke, T., Hay, G.J., Kelly, M., Lang, S., Hofmann, P., Addink, E., Feitosa, R.Q., van der Meer, F., van der Werff, H., van Coillie, F., Tiede, D., 2014. Geographic object-based image analysis-towards a new paradigm. ISPRS J. Photogramm. Rem. Sens. 87, 180–191.
Bruzzone, L., Carlin, L., 2006. A multilevel context-based system for classification of very high spatial resolution images. IEEE Trans. Geosci. Rem. Sens. 44 (9), 2587–2600.
Cardoso, J.S., Corte-Real, L., 2005. Toward a generic evaluation of image segmentation. IEEE Trans. Image Process. 14 (11), 1773–1782.
Castilla, G., Hay, G.J., Ruiz, J.R., 2008. Size-constrained region merging (SCRM): an automated delineation tool for assisted photo interpretation. Photogramm. Eng. Rem. Sens. 74 (4), 409–419.
Chen, G., Weng, Q., Hay, G.J., He, Y., 2018. Geographic object-based image analysis (GEOBIA): emerging trends and future opportunities. GISci. Rem. Sens. 55 (2), 159–182.
Chen, J., Li, J., Pan, D., Zhu, Q., Mao, Z., 2012. Edge-guided multiscale segmentation of satellite multispectral imagery. IEEE Trans. Geosci. Rem. Sens. 50 (11), 4513–4520.
Comaniciu, D., Meer, P., 2002. Mean shift: a robust approach toward feature space analysis. IEEE Trans. Patt. Anal. Mach. Intell. 24 (5), 603–619.
Costa, H., Foody, G.M., Boyd, D.S., 2018. Supervised methods of image segmentation accuracy assessment in land cover mapping. Rem. Sens. Environ. 205, 338–351.
Dey, V., Zhang, Y., Zhong, M., 2010. A review on image segmentation techniques with remote sensing perspective. In: Wagner, W., Székely, B. (Eds.), ISPRS TC VII Symposium – 100 Years ISPRS, XXXVIII (7A). IAPRS, Vienna, Austria, pp. 31–42.
Drăguţ, L., Csillik, O., Eisank, C., Tiede, D., 2014. Automated parameterisation for multi-scale image segmentation on multiple layers. ISPRS J. Photogramm. Rem. Sens. 88, 119–127.
Felzenszwalb, P.F., Huttenlocher, D.P., 2004. Efficient graph-based image segmentation. Int. J. Comput. Vis. 59 (2), 167–181.
Haris, K., Efstradiadis, S., Maglaveras, N., Katsaggelos, A., 1998. Hybrid image segmentation using watershed and fast region merging. IEEE Trans. Image Process. 7 (12), 1684–1699.
Hay, G.J., Castilla, G., Wulder, M.A., Ruiz, J.R., 2005. An automated object-based approach for the multiscale image segmentation of forest scenes. Int. J. Appl. Earth Observ. Geoinform. 7 (4), 339–359.
Hu, Z., Li, Q., Zhang, Q., Zou, Q., Wu, Z., 2017. Unsupervised simplification of image hierarchies via evolution analysis in scale-sets framework. IEEE Trans. Image Process. 26 (5), 2394–2407.
Huang, X., Zhang, L., 2008. An adaptive mean-shift analysis approach for object extraction and classification from urban hyperspectral imagery. IEEE Trans. Geosci. Rem. Sens. 46 (12), 4173–4185.
Johnson, B., Xie, Z., 2011. Unsupervised image segmentation evaluation and refinement using a multi-scale approach. ISPRS J. Photogramm. Rem. Sens. 66 (4), 473–483.
Li, D., Zhang, G., Wu, Z., Yi, L., 2010. An edge embedded marker-based watershed algorithm for high spatial resolution remote sensing image segmentation. IEEE Trans. Image Process. 19 (10), 2781–2787.
Liu, J., Li, P., Wang, X., 2015. A new segmentation method for very high resolution imagery using spectral and morphological information. ISPRS J. Photogramm. Rem. Sens. 101, 145–162.
Liu, Y.J., Yu, M., Li, B.J., He, Y., 2018. Intrinsic manifold SLIC: a simple and efficient method for computing content-sensitive superpixels. IEEE Trans. Patt. Anal. Mach. Intell. 40 (3), 653–666.
Ma, L., Li, M., Ma, X., Cheng, L., Du, P., Liu, Y., 2017. A review of supervised object-based land-cover image classification. ISPRS J. Photogramm. Rem. Sens. 130, 277–293.
Martin, D.R., 2003. An Empirical Approach to Grouping and Segmentation. Doctoral dissertation. Computer Science Division, University of California, Berkeley.
Ming, D., Li, J., Wang, J., Zhang, M., 2015. Scale parameter selection by spatial statistics for GeOBIA: using mean-shift based multi-scale segmentation as an example. ISPRS J. Photogramm. Rem. Sens. 106, 28–41.
Shackelford, A.K., Davis, C.H., 2003. A hierarchical fuzzy classification approach for high-

resolution multispectral data over urban areas. IEEE Trans. Geosci. Rem. Sens. 41 (9), 1920–1932.
Shi, J., Malik, J., 2000. Normalized cuts and image segmentation. IEEE Trans. Patt. Anal. Mach. Intell. 22 (8), 888–905.
Shih, F.Y., Cheng, S., 2005. Automatic seeded region growing for color image segmentation. Image Vis. Comput. 23 (10), 877–886.
Tilton, J.C., Tarabalka, Y., Montesano, P.M., Gofman, E., 2012. Best merge region-growing segmentation with integrated nonadjacent region object aggregation. IEEE Trans. Geosci. Rem. Sens. 50 (11), 4454–4467.
Trias-Sanz, R., Stamon, G., Louchet, J., 2008. Using colour, texture, and hierarchical segmentation for high-resolution remote sensing. ISPRS J. Photogramm. Rem. Sens. 63 (2), 156–168.
Vincent, L., Soille, P., 1991. Watershed in digital spaces: an efficient algorithm based on immersion simulations. IEEE Trans. Patt. Anal. Mach. Intell. 13 (6), 583–598.
Wang, M., Cui, Q., Wang, J., Ming, D., Lv, G., 2017. Raft cultivation area extraction from high resolution remote sensing imagery by fusing multi-scale region-line primitive. ISPRS J. Photogramm. Rem. Sens. 123, 104–113.
Wang, M., Dong, Z., Cheng, Y., Li, D., 2018. Optimal segmentation of high-resolution remote sensing image by combining superpixels with the minimum spanning tree. IEEE Trans. Geosci. Remote Sens. 56 (1), 228–238.
Wuest, B.Y., Zhang, Y., 2009. Region based segmentation of QuickBird multispectral imagery through band ratios and fuzzy comparison. ISPRS J. Photogramm. Rem. Sens. 64 (1), 55–64.
Xiao, P., Feng, X., An, R., Zhao, S., 2010. Segmentation of multispectral high-resolution satellite imagery using log Gabor filters. Int. J. Rem. Sens. 31 (6), 1427–1439.
Yang, J., He, Y., Caspersen, J., 2017. Region merging using local spectral angle thresholds: a more accurate method for hybrid segmentation of remote sensing images. Rem. Sens. Environ. 190, 137–148.
Yu, Q., Clausi, D.A., 2008. IRGS: Image segmentation using edge penalties and region growing. IEEE Trans. Patt. Anal. Mach. Intell. 30 (12), 2126–2139.
Zhang, Y., 2002. Problems in the fusion of commercial high-resolution satellite images as well as Landsat 7 images and initial solutions. Int. Arch. Photogramm. Remote Sens. 34 (Part 4).
Zhang, H., Fritts, J.E., Goldman, S.A., 2008. Image segmentation evaluation: a survey of unsupervised methods. Comput. Vis. Image Underst. 110 (2), 260–280.
Zhang, X., Xiao, P., Song, X., She, J., 2013. Boundary-constrained multi-scale segmentation method for remote sensing images. ISPRS J. Photogramm. Rem. Sens. 78, 15–25.
Zhang, X., Xiao, P., Feng, X., Wang, J., Wang, Z., 2014. Hybrid region merging method for segmentation of high-resolution remote sensing images. ISPRS J. Photogramm. Rem. Sens. 98, 19–28.
Zhang, X., Feng, X., Xiao, P., He, G., Zhu, L., 2015. Segmentation quality evaluation using region-based precision and recall measures for remote sensing images. ISPRS J. Photogramm. Rem. Sens. 102, 73–84.